Bureau
International des
Poids et
Mesures

Guide to the Realization of the ITS-90

1 édition 2018

Partie 2
Part 2

Fixed Points: Influence of Impurities

January 01, 2018
01 janvier 2018

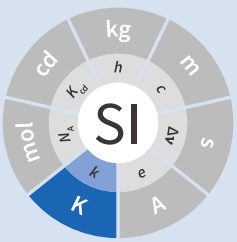

Bureau International
des Poids et Mesures

Guide to the Realization of the ITS-90
Part 2: Fixed Points: Influence of Impurities

1st edition 2018

01 January 2018

Abstract

This paper is a part of guidelines, prepared on behalf of the Consultative Committee for Thermometry, on the methods how to realize the International Temperature Scale of 1990.

It discusses all major issues linked to the influence of impurities on fixed-point temperatures for the realization of the International Temperature Scale of 1990.

1. Introduction

The fixed-point temperatures of the ITS-90 are defined for phase transitions (triple, melting, and freezing points) of ideally-pure, single-component substances (with the exception of water, single-element substances). Though the impurity content of fixed-point samples approaches or exceeds a level of one part per million (1 ppm) mole fractions, the component caused by the influence of impurities often dominates the uncertainty budgets of fixed-point realisations. Underestimation of this component may be the root cause of temperature differences in excess of their combined uncertainties among the national metrology institutes, as demonstrated in CCT Key Comparisons [51], [59]. The lack of a common approach created a situation whereby estimates of this single component differed by orders of magnitude from lab to lab even though the materials and their treatment are very similar.

Recent improvements in the accuracy and limits of detection in the chemical analysis of impurities in fixed-point substances have made it feasible to model and correct for some impurities. This has had a considerable impact on both the realisation techniques (see *Guide* Sections 2.2 Triple Point of Water to 2.5 Fixed Points for Radiation Thermometry) and uncertainty analysis. This *Guide* Section 2.1 deals only with impurity effects. However, the same observations and models apply to dilute isotopic effects. At the state-of-the-art level of uncertainty, varying isotopic compositions among fixed-point samples for the hydrogen, neon, and water fixed points result in significant variations in the realised temperatures. To solve this problem (for these three substances), the isotopic compositions are specified in the Technical Annex for the ITS-90 [TA-ITS-90 2017] together with functions for correcting the realised temperatures to the reference compositions.

In this section, it is intended to standardise the methodology by proposing the Sum of Individual Estimates (SIE) as the preferred method for estimating the change in the observed liquidus-point temperature relative to that of the chemically-pure material when sufficient information is available to enable the required calculations. For this reason, it is strongly recommended that a good quality chemical assay of the fixed-point substance is obtained when a new fixed-point cell is constructed or purchased. The assay should have a detection limit of the order of 10 parts per billion, and should cover the widest possible range of elements. When this is not possible, the Overall Maximum Estimate (OME) is an acceptable, though less desirable, alternative. Uncertainty Estimation based on Representative Comparisons (ERCs) is specifically discouraged, but ERCs remain useful as a tool to assess in-ingot impurity effects. Thermal analysis (i.e. as derived from the slope of a freezing or melting curve) is another means of validation. However, thermal analysis should not be used to derive the fixed-point-cell uncertainty component attributable to impurities because e.g. some impurities can alter the melting temperature without broadening the melting range.

The section is organised as follows. First, the crystallographic behaviour of impurities during freezing and melting under different experimental conditions is briefly discussed in the dilute limit. Then, methods are recommended for estimating the influence of impurities on the phase-transition temperature and the corresponding uncertainties. Here, special emphasis is given to considering only those impurities that actually influence the phase-transition temperature. General comments are given on the crystallographic parameters needed to apply these methods, on the traceable analysis of the impurity content, and on the assessment of the degrees of freedom required when expanded uncertainties are to be deduced for a given confidence level. This is followed by a description of methods to validate fixed-point cells. Finally, the peculiarities of the impurity effects in three classes of fixed-point substances are

compared: cryogenic gases (triple points of *e*-H_2, Ne, O_2, and Ar); water; and metals (triple point of Hg, melting point of Ga, and freezing points of In, Sn, Zn, Al, Ag, Au, and Cu).

2. Effects of impurities in fixed-point samples

Background information on the behaviour of impurities during freezing and melting is contained in various text books, for instance in [48], [32], [96], [76], [74], [13], [38], [15], [83], [45], [75], [20]. The starting point for the thermodynamic description of phase transitions is establishing the equality of the thermodynamic potentials of the involved phases. In Appendix 1, this approach is used to derive approximate relations between the basic crystallographic parameters and the relevant thermodynamic quantities. In this subsection, the relations from the literature that are needed to assess the uncertainty due to the influence of impurities are summarised.

2.1. Basic crystallographic parameters

In order to assess the quality of the realized phase-transition temperature of a fixed-point material, one must analyse in detail the influence of the concentrations of the material's impurities (and their segregation) on the fixed-point temperature and on the shape of the freezing and melting curves, see for instance [27]. This influence is governed primarily by the crystallographic behaviour of the impurities at low concentrations in the host material. From the equilibrium binary phase diagram at low concentrations, see Chapter 4, one must deduce for each impurity the following two parameters: the equilibrium distribution coefficient, $k_0^i = c_s^i / c_1^i$, of impurity i and the derivative $m_1^i = \partial T_l / \partial c_1^i$ of the temperature of the liquidus line in the phase diagram with regard to the concentration of impurity i, where c_s^i and c_1^i are mole fraction concentrations of the impurity i in the solid and liquid equilibrium phases of the sample, respectively. The equilibrium distribution coefficient is a measure of the relative solubility of the impurity in the solid and liquid phases of the host. For different solubilities ($k_0^i \neq 1$), solid will form with a different impurity concentration relative to the liquid as freezing progresses. This segregation of impurities between the solid and liquid phases causes the concentration in the remnant liquid to increase ($k_0^i < 1$) or decrease ($k_0^i > 1$), which in turn causes the phase-transition temperature to decrease with increasing solid fraction in both cases. The solubility in the solid host is negligible if the equilibrium distribution coefficient has a value ≤ 0.01. The shape of an observed phase-transition curve may depend strongly on the experimental conditions, especially on the rate of freezing, if the concentration of impurities is significant. In some cases, details of the history of the sample before it enters the phase transition, such as the length of time in the liquid state and the temperature of the liquid before beginning the freeze, may also be important.

2.2. Pure Solid / Liquid Solution

For the rare case when all impurities are insoluble in the solid phase of the host material ($k_0^i = 0$) and the ideal solution law is valid, the impurities remain in the liquid solution. Then, if one assumes that there are no concentration gradients in the liquid as the host component slowly freezes, the depression of the freezing-point temperature (relative to the freezing-point temperature of the pure material) is directly proportional to the impurity concentration divided by the "first cryoscopic constant" [33], [30], [53], [31]. This is expressed approximately as

$$T_{\text{pure}} - T_{\text{obs}} = c_1 / A, \tag{1}$$

T_{obs} is the observed equilibrium temperature of the sample. When an infinitesimalamount of solid has frozen, T_{obs} is the liquidus-point temperature of the sample. T_{pure} is the freezing-point temperature of the pure material, c_1 is the mole fraction impurity concentration in the liquid, and A is the first cryoscopic constant. A is given by the relation:

$$A = L/\left(R[T_{pure}]^2\right), \tag{2}$$

where L is the molar heat of fusion and R is the molar gas constant.

Ideally, as freezing proceeds, the pure solid phase of the fixed-point substance remains in equilibrium with the impure liquid phase (a solution of the fixed-point substance and the impurity), and the impurity concentration c_1 is inversely proportional to the fraction F of the sample melted, i.e.

$$c_1 = c_{11}/F, \tag{3}$$

where c_{11} is the impurity concentration when the fixed-point material is completely melted ($F = 1$). By substitution of Equation (3) into Equation (1), the following equation is obtained

$$T_{pure} - T_{obs} = c_{11}/(FA) \tag{4}$$

The effect of the total impurity concentration c_{11} is thus enhanced by the factor $1/F$. This is often called Raoult's law.

Thus, for systems containing only impurities with $k_0^i = 0$, plots of temperature versus $1/F$ provide a direct measure of the impurity concentration, and extrapolations to $1/F = 0$ can be used to determine T_{pure}. In practice, few impurities have $k_0^i = 0$ exactly, and it is extremely unlikely that a fixed point will only have impurities with $k_0^i = 0$, so Equation (4) is at best an approximation for some fixed-point realisationsand misleading for others. If Equation (4) is fitted to freezing curves of samples containing many different impurities with a range of k_0^i values, the fit is only approximate, tends to confuse temperature elevation and depression, and can significantly underestimate the temperature depression in samples with significant impurity concentrations with $0.1 < k_0^i < 1$ [25], [27].

2.3. Solid Solution / Liquid Solution

When solid solutions of a fixed-point material and its impurities are formed (solid solution / liquid solution), three distinct conditions of segregation of the components can occur during freezing (diffusion in the solid phase can usually be neglected) [32]: Complete mixing, partial mixing, and no mixing in the liquid. In the latter two cases, non-equilibrium effects have to be considered. In practice, several non-equilibrium effects affect the distribution of impurities. These include diffusion, convection, and the non-uniform advancement of the interface due to the formation of particular crystalline structures [83].

For fixed-point realisations, diffusion effects are particularly significant. The time taken for impurities to fully diffuse and equilibrate over distances of many millimetres in the liquid phase is usually tens of hours. Consequently, the shape and temperature range of freezing plateaus can depart significantly from the equilibrium curves. The effects of convection are insignificant because of the very small temperature gradients in the sample volume. Considering the typical order of magnitude of the diffusion coefficients D in liquid metals ($10^{-5}\,cm s^{-1}$), the case of complete mixing is approximated only at very small rates of freezing, i.e., at very low velocities v of the liquid/solid interface ($vl/D << 1$, where l is

the length of the sample in the freezing direction, i.e., the direction of solid growth). Thus, for the experimental conditions normally realized, the results must be analysed carefully to determine whether the segregation of the impurities is in accordance with the strongest possible dependence given by Equation (5) below.

2.3.1. Complete mixing in the liquid

For this case, it is assumed that freezing is slow enough for complete and uniform mixing (resulting from convection and diffusion of the impurities in the liquid phase) to preclude concentration gradients in the liquid. This leads to the maximum possible segregation of the impurities, and the dependence of T_{obs} on F is given by the following equation based on the Gulliver-Scheil model [34], [82], [74]

$$T_{\mathrm{pure}} - T_{\mathrm{obs}} = -\sum_i m_1^i c_1^i\,(F) = -\sum_i m_1^i c_{11}^i F^{k_0^i - 1}. \tag{5}$$

Equation (4) results from Equation (5) if $k_0^i = 0$ and $m_1^i = -1/A$ for all impurities. For $k_0^i = 1$, no segregation of impurities occurs, and T_{obs} is independent of F.

For many systems, it has been shown experimentally [38] that the relation

$$\partial T_1 / \partial c_1^i = -\left(1 - k_0^i\right)/A \tag{6}$$

is a good approximation at low concentrations, cf. Appendix 2 and [70], [71]. In Appendix 1,this relation is derived from the thermodynamic description of phase transitions and by assuming that the impurity-host mixtures are ideal solutions and the heat of fusion is independent of the impurity concentrations.

2.3.2. Partial mixing in the liquid

For the case of partial mixing in the liquid, the distribution of impurities in the liquid is affected by diffusion and convection. Under these assumptions, the segregation of impurities depends strongly on the freezing conditions and is governed by an effective distribution coefficient k_{eff}^i that has a value between k_0^i and 1. For a planar solid-liquid interface in an infinite liquid, it is given by [14], [74]

$$k_{\mathrm{eff}}^i = \frac{k_0^i}{k_0^i + \left(1 - k_0^i\right)\,\exp\left(-v d / D^i\right)} \tag{7}$$

where v is the interface velocity, d is the $1/e$ thickness of the liquid layer in front of the interface where the impurity has become enriched or depleted, and D^i is the diffusion coefficient for the impurity in the liquid. The value of k_{eff}^i approaches 1 if the rate of freezing and, consequently, the velocity of the liquid/solid interface, is high [32]. When the freeze happens very quickly relative to diffusion rates, no segregation is observed and the entire sample freezes at one temperature. Thus, the effect of rapid freezing during quenching is to prevent segregation. (The limited thermal conductivity of materials makes it practically impossible to freeze fixed-point samples sufficiently quickly to prevent segregation completely [43].) Therefore, to properly analyse the influence of impurities, it is very important to ensure conditions are such that k_{eff}^i has nearly the same value as k_0^i.

2.3.3. No mixing in the liquid

For this case, it is assumed that the impurity distribution in the liquid phase is affected by diffusion alone, and that diffusion is inadequate to mix the impurities throughout the liquid. Then, as freezing advances, the impurity concentration in the liquid layer adjacent to the liquid/solid interface increases ($k_0^i < 1$) or decreases ($k_0^i > 1$) as the impurities are rejected from or gathered by the freezing solid. In an infinite sample, this progresses until the concentration of impurities freezing into the solid is c_{11}^i (the steady-state impurity distribution). Under those conditions, the concentration of impurities in the liquid at the interface will be c_{11}^i/k_0^i and there will be no further segregation. For a finite-size fixed-point sample, the resulting impurity distribution in the solid depends strongly on the equilibrium distribution coefficient, the rate of freezing (velocity of the liquid/solid interface), the diffusion coefficient of the impurity in the liquid, and the sample geometry [84], [93], [97]. For the discussion here, the special freezing conditions that occur in the case of no mixing may be represented by the simple equation given in [92] that describes the resulting impurity distribution in the solid:

$$c_s^i = c_{11}^i\left[1-\left(1-k_0^i\right)\ \exp\ \left(-k_0^i v x/D^i\right]\right., \tag{8}$$

where x is the distance of the liquid-solid interface from the location where freezing commenced.

2.3.4. Melting curves

The discussions above apply directly only to freezing. When evaluating melting curves, a principal difference between freezing and melting has to be considered [27], [105]: Due to supercooling, freezing occurs at, and grows from, the interfaces created by the initial nucleation of solid, whereas the absence of overheating allows melting to occur also in microscopic regions throughout the whole solid sample portion. In these microscopic regions, diffusion may be sufficient to redistribute the impurities, i.e. melting in the microscopic regions takes place nearly under equilibrium conditions in the volume. Near thermal equilibrium, melting starts in microscopic sample portions having a depressed melting temperature, i.e. near crystal defects (e.g. grain boundaries—representing inner surfaces—and dislocations) and surfaces [62].

The micro-redistribution is necessary for the beginning of the melt in the vicinity of the solidus line because the liquid phase is unstable with a macroscopically uniform impurity concentration at the temperature defined by the solidus line. Stability demands a liquid with an equilibrium impurity concentration equal to c_s^i/k_0^i. The situation is illustrated in Figure 1 for an impurity with $k_0^i < 1$. Equilibrium freezing at low velocities is possible starting at the liquidus line as shown in the left diagram because mixing in the liquid is sufficient. The impurity concentrations in the solid (solidus line) and liquid (liquidus line) can have the ratio k_0^i. On the contrary, macroscopic diffusion in the solid is too slow for an equilibrium melting starting at the solidus line. Thus, macroscopic melting can take place only at the liquidus line, but this is a non-equilibrium phase transition. Equilibrium melting along the dotted line in the right diagram is restricted to microscopic regions.

During melting, the thermometer measures the temperature of the material adjacent to the re-entrant thermometer well of the fixed-point cell that is determined by the temperature of the interfaces between the microscopic liquid drops and the surrounding solid. The temperature of the advancing macroscopic outer solid-liquid interface is slightly higher than that measured by the thermometer because at this interface non-equilibrium melting takes place at the

liquidus line. The outer interface reflects the impurity distribution resulting from the freeze that precedes the melt, but this has no influence on the thermometer reading. Thus, the melting curves of rapidly frozen samples are not fully flat because of the microscopic segregation. After slow freezing, the macroscopic segregation superposes the microscopic one. An observed melting curve is, therefore, not a time-reversed version of the freezing curve, and it is generally broader. This is the reason why freezing curves are mostly the better choice for fixed-point realisations.

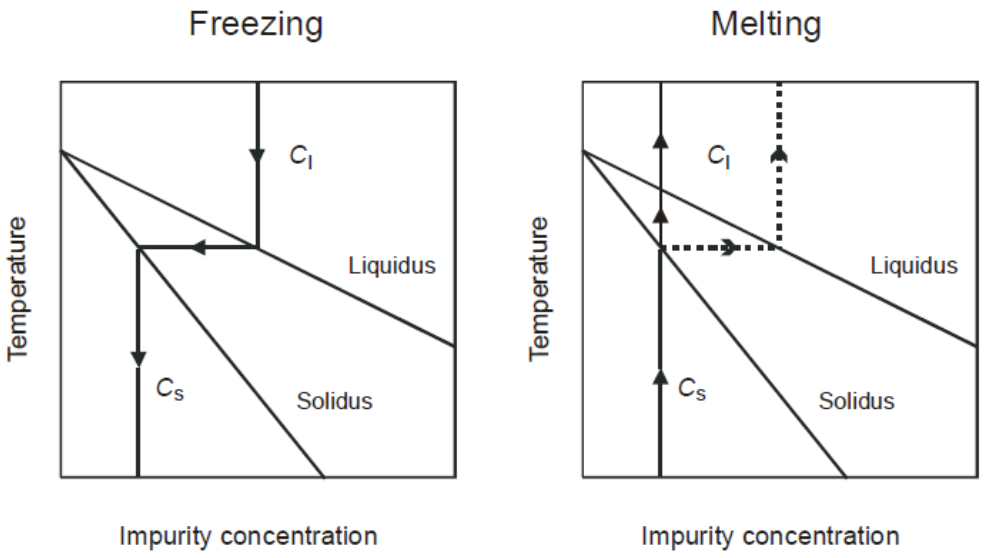

Figure 1 — Simplified schematic representation of freezing (on the left) and melting (onthe right) in a binary phase diagram for an impurity with $k_0^i < 1$ at low concentrations. For macroscopic phase changes, only the way along the solid lines is allowed. The dotted melting line is possible in microscopic regions.

Furthermore, a reliable evaluation of a melting curve obtained after a slow freeze is nearly impossible because the distribution of impurities and the location of the liquid-solid interfaces are ambiguous for the following reason. Impurities with $k_0^i < 1$ are concentrated by the freezing process from the outer to the inner cell wall near the re-entrant thermometer well. During the melt, a liquid-solid interface may form in this impure zone even without inducing it, and the thermometer measures the temperature of this zone as this interface sweeps slowly through the layers of impurity. Under these conditions, the observed melting behaviour may correspond to that of only a few percent of the sample.

3. Methods for estimating the effects of impurities and uncertainties

Three methods of differing significance were proposed in [26], [28] with a view to obtaining a reliable estimate of the uncertainty component due to impurities. These methods are the "Sum of Individual Estimates" (SIE), the "Overall Maximum Estimate" (OME), and the "Estimate based on Representative Comparisons" (ERC). They are discussed here in turn (ERC in Chapter 7, see p. 23), and also some additional combined approaches. Since the estimates are valid for the liquidus point, where only an infinitesimal portion of the sample is frozen, the determination of the liquidus-point temperature is treated at the end of this section.

3.1. Sum of individual estimates (SIE)

The application of this method requires the determination of the concentrations c_1^i of all relevant impurities using appropriate analysis techniques, see Chapter 5, and knowledge of the concentration-dependence of the fixed-point temperature for the different impurities detected. The latter is simply the derivative $m_1^i = \partial T_1/\partial c_1^i$ of the temperature T_1 of the liquidus line in the phase diagram with regard to the concentration of impurity i, which must be deduced for each impurity from the corresponding equilibrium phase diagram at low concentrations (see Chapter 4, see p. 19), and c_1^i is the mole fraction concentration of the impurity i in the liquid equilibrium phase of the sample. In Appendix 2 *Distribution coefficients and liquidus-line slopes*, the derivatives are tabulated together with the distribution coefficients for each of the fixed points of the ITS-90. The intent of this collation of data is to harmonise the uncertainty estimation and avoid duplication of analysis of the phase diagrams. The Appendix 3 *Data on precipitation* and Appendix 4 *Common impurities found in fixed-point materials* remaina work in progress that will be updated as additional information becomes available. Use of the SIE method is not recommended for materials of less than 99.999% purity since the assumptions of independent influence appropriate to the dilute limit may no longer apply.

Based on Equation (5), the SIE approach yields for the change in the observed fixed-point temperature T_{obs} relative to that of the chemically pure material T_{pure} at the liquidus point ($F = 1$, where F is the fraction of sample melted):

$$\Delta T_{\mathrm{SIE}} = T_{\mathrm{pure}} - T_{\mathrm{obs}} = -\sum_i c_{11}^i \left(\partial T_1/\partial c_1^i\right) = -\sum_i c_{11}^i m_1^i. \tag{9}$$

In Equation (9), c_{11}^i is the concentration of the impurity i at the liquidus point. The summation is over all impurities present in the liquid since, in the dilute limit, there is evidence that each impurity behaves independently, and the formation of ternary and higher-order compounds exert a negligible influence. Thus, the SIE method is in explicit accordance with the notion that the temperature of the fixed point should be *corrected* for the influence of impurities by the amount calculated via Equation (9). This is fully consistent with the directive in the *Evaluation of measurement data — Guide to the Expression of Uncertainty in Measurement* (GUM) [JCGM 2008] that calls for all measurements to be corrected for known bias or systematic effects. At present, the uncertainty estimates for chemical analyses are rarely expressed in a manner consistent with the GUM and the reliability of the estimates remains a concern, see Chapter 5.

The standard uncertainty of the estimate ΔT_{SIE} then results from the uncertainties of the analysis data $u\left(c_{11}^{i}\right)$ and of the data for the concentration dependencies $u\left(m_{1}^{i}\right)$:

$$u^2\left(\Delta T_{\mathrm{SIE}}\right)=\sum_{i}\left[u\left(c_{11}^{i}\right)m_{1}^{i}\right]^2+\left[c_{11}^{i}u\left(m_{1}^{i}\right)\right]^2. \tag{10}$$

When the uncertainty of the chemical analysis is large compared to other uncertainties, it is imperative to compute the degrees of freedom associated with the standard uncertainty of Equation (10), see Chapter 6, to ensure that the expanded uncertainty can be properly computed.

It is challenging to implement the SIE method in practice because of the following reasons:

- limitations of the chemical analysis;
- limited knowledge of low-concentration liquidus-line slopes;
- the chemically analysed sample portion may not be representative of the ingot in the fixed-point cell, e.g. due to a contamination of the material during the filling and use of the cell;
- limited knowledge of the effect of oxides formed throughout the ingot and effect of other gases.

Therefore, complementary techniques are recommended to validate fixed-point cells, see Chapter 7. If the necessary information is not available for all impurities, the SIE method can be combined with other approaches, see Section 3.3.

In the correction ΔT_{SIE} of the SIE approach given by Equation (9), only impurities dissolved in the fixed-point material should be included. Appendix 4 *Common impurities found in fixed-point materials* lists the impurity elements that are most likelyto be present in commercially-available materials. In [23], [24], the authors argued that some impurities may be present as undissolvedoxides, and should be omitted from the correction. An elemental chemical analysis (e.g. Glow Discharge Mass Spectrometry (GD-MS)) is incapable of providing evidence of such compounds. The formation of impurity oxides is likely if the impurity's affinity for oxygen exceeds that of the host material. As a rough guide for the metallic fixed-point materials of the ITS-90, in [23] a ranking is deduced by comparing thermodynamic data for many impurity oxides to that for the oxides of the host metals (this is analogous to the electromotive series). This ranking should be applied with caution for the following reasons.

1. The ranking is based on estimates of chemical activities, which may strongly deviate from the concentration values.
2. There needs to be sufficient oxygen at the sites of the impurity atoms.
3. The impurity molecules must precipitate to an inner or outer surface. If the oxide molecules are soluble in the melt, but not in the solid host metal, then these molecules have an influence corresponding to Raoult's law, i.e. possibly a stronger influence than the impurity atoms, or at least different.

Items 2) and 3) are connected with the process kinetics. Further investigations are necessary because the ranking is not conclusive for several impurity oxides due to the lack of data. As well, the behaviour of non-metallic elements and gases is difficult to estimate [Drápala and Kuchař 2008]. (For instance, the effect of dissolved oxygen on the silver freezing point is discussed by Bongiovanni *et al.* (1975).) Thus, the exclusion of certain impurities from the correction ΔT_{SIE} makes the application of the SIE method easier, but it must be based on sound evidence. If this cannot be guaranteed, it is better to apply combined estimation methods, see

below. The conditions that exist during doping experiments are quite different from those that occur during a typical fixed-point realization, so they do not yield conclusive results per se.

For instance, active mixing of the components (e.g. by stirring) may introduce additional oxygen. Data on the possibility of precipitation are collated in Appendix 3.

The SIE method can be applied to the cryogenic fixed points (triple points of *e*-H_2, Ne, O_2, and Ar) because the cryogenic gases have relatively few impurities that affect the liquidus-point temperature, and most of the liquidus-line slopes are well known, see [63], [66], Section 8.1, and Appendix 2. Furthermore, the typical maximum magnitude of the effects (a few 10 μK per ppm) is an order of magnitude smaller than for metal fixed points. The SIE method is not yet fully applied to any of the metal fixed points. Fellmuth and Hill (2006) presented the first example of an SIE analysis for a metal fixed point, namely the freezing point of tin. (They have omitted six non-metallic elements and gases detected by mass spectrometry.) Furthermore, they discussed and demonstrated the limitations of thermal analysis in the assessment of impurity effects, and compared the SIE method to other methods. This has been done also by other groups, see Chapter 7. Other examples for the application of the SIE method are given in [11], [77], [44].

3.2. Overall maximum estimate (OME)

The OME method must be applied if the concentrations of the impurities or their individual influence on the fixed-point temperature are unknown as accurately as necessary for the SIE method to be of use. All that is required is an accurate estimate of the overall impurity concentration, expressed as a mole fraction. With this, the OME for the liquidus-point temperature change is given by

$$\Delta T_{\mathrm{OME}} = c_{11}/A. \tag{11}$$

For the fixed-point substances of the ITS-90, values for the first cryoscopic constant A are given in Table 1 together with the latent heats of fusion L. At the liquidus point ($F = 1$), the right side of Equation (11) is equal to that of Equation (4), but this does not mean that the validity of Raoult's law is assumed. ΔT_{OME} can be regarded as a maximum estimate because the manufacture of high-purity metals usually includes zone refining, which preferentially removes impurities with extreme values of the equilibrium distribution coefficient ($k_0^i > 2$). With Equation (6) this means: The derivative m_1^i is not larger than $1/A$, and Equation (11) follows from Equation (9) for $m_1^i = -1/A$. (Nevertheless, it is recommended that the concentration of impurities with $k_0^i > 2$ be verified, as only a small number are relevant to each fixed-point substance.)

Even though the OME method provides an overall estimate for the expected temperature change, it should not be used to correct the fixed-point temperature because Equation (11) yields only a bound. However, the value may be used to estimate the uncertainty component arising from the impurities present in the sample. If it is assumed that any liquidus temperature from $-\Delta T_{\mathrm{OME}}$ to T_{OME} is equally likely, Equation (12) is recommended for this purpose:

$$u^2(\Delta T_{\mathrm{OME}}) = [\Delta T_{\mathrm{OME}}]^2/3 = [c_{11}/A]^2/3. \tag{12}$$

Especially when the uncertainty $u(\Delta T_{\mathrm{OME}})$ is large compared to other components of the overall uncertainty budget, it is again necessary to determine the effective degrees of freedom. The finite degrees of freedom arise principally from the uncertainty in the estimated impurity

concentration c_{11}. Given that the uncertainty of the impurity is likely to be in the range 100% to 300%, see Chapter 5, it is vital that the degrees of freedom be stated together with the standard uncertainty to ensure proper calculation of the coverage factor and expanded uncertainty for the desired confidence level, see Chapter 6.

If the uncertainties of the analysis results and the slopes m_1^i are sufficiently small, the SIE method generally yields smaller uncertainty estimates than the OME method.

Chemical assays should include, as a minimum, all of the common elements that are normally found in a particular fixed-point material, see Appendix 4. If the abundances of these elements are not specifically identified, then half the detection limit should be used. It is important to emphasize that the certificate of analysis must include an uncertainty statement as the chemists performing the analyses are in the best position to make such estimates. When such information is lacking, or when it is evident that the analysis is incomplete, use of the nominal purity (e.g. 99.9999%) is recommended with an estimated standard uncertainty equal to the remaining impurity (e.g. 10^{-6} mole fraction or ppm). However, use of the nominal purity can be expected to underestimate the uncertainty component.

Table 1. The latent heats of fusion (L) and the first cryoscopic constants (A) for thefixed-point substances of the ITS-90 [79].

Substance	T_{90}	L	A	A^{-1}
	K	$Jmol^{-1}$	K^{-1}	$mK/10^{-6}$ mole fraction
e-H_2	13.8033	117	0.0739	0.014
Ne	24.5561	335	0.0668	0.015
O_2	54.3584	444	0.0181	0.055
Ar	83.8058	1188	0.0203	0.049
Hg	234.3156	2301	0.005041	0.198
H_2O	273.1600	6008	0.009684	0.103
Ga	302.9146	5885	0.007714	0.130
In	429.7485	3291	0.002143	0.467
Sn	505.078	7162	0.003377	0.296
Zn	692.677	7068	0.001772	0.564
Al	933.473	10789	0.001489	0.672
Ag	1234.93	11284	0.000890	1.124
Au	1337.33	12720	0.000855	1.170
Cu	1357.77	12928	0.000843	1.186

3.3. Combined methods

To reduce the effort in estimating the uncertainty due to impurities, it may be acceptable to combine methods. An obvious combination is to use the SIE method (correction and uncertainty estimate) for the dominant impurities and the OME method (only the uncertainty estimate) for the remaining impurities.

It is also possible to use the SIE method together with a modified OME method if the equilibrium distribution coefficients of all relevant impurities are known. The modification

of the OME method concerns the estimation of the overall concentration of the remaining impurities, which should have k_0^i values less than or approximately equal to 0.1. The change of the liquidus temperature by these impurities can be reliably estimated by fitting the right-side expression of Equation (4) to a freezing or melting curve measured with one solid-liquid interface, see [52], in an appropriate F range. (The fitted coefficient c_{11} is also influenced by the dominant impurities with k_0^i values larger than 0.1 present in the sample, but this usually leads to an acceptable overestimation.) Thus, it is only necessary to determine the concentrations of the impurities with $k_0^i > 0.1$ and to combine the two uncertainty estimates based on Equation (12) ($k_0^i \leq 0.1$) and Equation (10) ($k_0^i > 0.1$).

It must be stressed that Equation (4), i.e. Raoult's law, should not be applied casually for all impurities since, strictly speaking, it is only valid for impurities that are insoluble in the solid phase ($k_0^i = 0$). A chemical analysis is required to ensure that the influence of impurities with significant solubility in the solid phase is first accounted for by the SIE method. For $k_0^i > 0.1$, the inappropriate application of Raoult's law will significantly underestimate the change in the liquidus-point temperature [25], [27].

Since the modified OME method depends on fitting the freezing or melting curve over some range of liquid fraction F, the results so obtained will be affected by other factors that influence the shape of the curve. Care must be taken that the realisation follows good practice to minimize the effects of the thermal environment on the shape of the curve [52], [80], [22], [67], [68]. While the origin of the slope of the melting curve may beincorrectly attributed (when such effects are observable), the uncertainty arising from the analysis goes some way towards recognizing the fact that such curves are not ideally flat, and the likely consequence is a somewhat increased uncertainty estimate. Furthermore, non-equilibrium effects have to be considered when evaluating freezing or melting curves, see Section 2.3. While long freezing curves are preferred, investigations of the rate-dependence are encouraged as such influences ought to be part of the overall uncertainty budget. This investigation allows an estimate of how large the deviations from the behaviour corresponding to Equation (4) may be. It has long been recognized that the shape of the melt is sensitive to the distribution of impurities, see Section 2.3.4. This is best demonstrated by comparing a melt following a very fast (quench) freeze that generally leads to a reasonably homogeneous sample to one following a very slow freeze that allows significant impurity segregation.

Two other modifications of the OME method are proposed in [65]. The *One-Sided OME* is simply a proposal to decrease the uncertainty estimate by a factor oftwo compared with Equation (12) if all relevant impurities have equilibrium distribution coefficients smaller than one. The *Average Overall Estimate* uses in Equation (11) the mean liquidus-line slopes of all relevant impurities instead of $1/A$. Both approaches decrease the uncertainty estimate, but do not contain more information on the impurity effects. The schemes IE-IRE and SIE-IE-IRE proposed by Bloembergen *et al.* (2011), where the acronym IE stands for *Individual Estimates* and IRE for *Individual Random Estimates*, are not really new approaches. In fact, IE is identical with SIE if Equation (6) is used for determining approximate values of the liquidus-line slopes $m_1^i = \partial T_1 / \partial c_1^i$. After a complicated derivation, the final formula for IRE is completely identical with Equation (12) of the OME method. Thus, IE-IRE is SIE-OME applying Equation (6) as approximation.

3.4. Determination of the Liquidus-Point Temperature

Complications from non-equilibrium effects, multiple impurities of different k_0^i values acting together, and thermal effects make it practically impossible to definitively relate the observed broadening of freezing or melting curves to impurity concentrations or to infer reliable quantitative estimates of the temperature depression or elevation. Consequently, the only point on a phase-transition curve amenable to modelling (from which the fixed-point temperature is determined) is the liquidus point.

For the freezing curves of the metallic fixed-point materials, the maximum should be taken as the best approximation of the liquidus-point temperature. Observation of the curves should be performed with inner and outer liquid-solid interfaces (see [52], see p. 30) and should extend past the maximum by 10 % to 20 % of the fraction frozen, to clearly establish the value of the maximum and the resolution of its determination. Furthermore, it should be checked if special freezing conditions could cause a significant difference between maximum and liquidus-point temperature, see for instance [106].

For the melting curves used to realize the triple points of the cryogenic gases via adiabatic techniques as well as the triple point of mercury and the melting point of gallium, the liquidus-point temperature should be determined by extrapolating the dependence of the melting temperature on the fraction of sample melted to the liquidus point. This is done by fitting a function $T_{\mathrm{obs}}(F)$ to the experimental data, keeping in mind the following suggestions:

- The fitting should be performed in an F range for which the melting temperature T_{obs} of the fixed-point sample can be determined with the lowest possible uncertainty. For example, the cryogenic gases have very small thermal conductivities. This causes the melting curves to become sensitive to the thermal surroundings as melting proceeds towards large F values. This influences the shape of the melting curve and increases the uncertainty in estimating the liquidus–point temperature. On the other hand, most physical effects influence the melting temperature at low F values where the solid phase dominates (i.e. effects arising from the influence of crystal defects, of the spin-conversion catalyst necessary to realize the triple-point of equilibrium hydrogen (e-H_2), etc.). Thus, the choice of the F range used for fitting should be considered very carefully after taking into account the properties and behaviour of the specific fixed-point material [29].
- To extrapolate the melting curve to the liquidus point, the melting curve is approximated by a function $T_{\mathrm{obs}}(F)$ whose form corresponds to the F-dependence of the effects influencing the shape of the melting curve. (The simplest approaches are to fit T_{obs} versus F or $1/F$.) The optimum function may prove different for the various fixed-point materials. The choice should be guided by selecting a form that minimizes the standard deviation of the experimental data from the fit function and maximizes the repeatability of the liquidus-point temperature.

Fortunately, the melting curves of high-purity materials are in many cases sufficiently flat that detailed fitting is unnecessary. The value near 50% melted fraction is often an adequate estimate of the liquidus-point temperature that avoids the influences of crystal defects, etc. at low melted fraction and the thermal influences that manifest at large melted fraction. This approach is recommended for the very flat curves observed for the fixed points of mercury, water, and gallium realizable at very high purity.

The uncertainty in determining the liquidus-point temperature from the observed freezing or melting curves must also be included in the overall uncertainty budget for the fixed-point realisation. This component is in addition to the uncertainty component attributable

to the influence of impurities on the liquidus-point temperature and estimated as discussed previously.

4. Collation of Crystallographic Parameters

The parameters m_1^i and k_0^i necessary for the estimation of impurity effects can be deduced via three paths: Binary phase diagrams published in the literature, thermodynamic calculation of phase equilibria, and doping experiments at low impurity concentrations. These three paths are discussed below in turn. A review of the available data on equilibrium distribution coefficients k_0^i is given in [70], cf. Appendix 2.Suggested k_0^i values are deduced from different sources and evaluations:experimental literature data, thermodynamic calculations, application of Equation (6), predictions based on patterns for the dependence of k_0^i on the position of the host material in the periodic table, and the Goldilocks principle [6], [99] for estimating the correct value within an order of magnitude. Surprisingly, the data evaluation in [70] seems to indicate that the distribution coefficient of an impurity is independent of the properties of the host material. Furthermore, useful guidance on the magnitude of this parameter is given.

The data used to construct phase diagrams has improved significantly in recent years. In 1978, the ASM (American Society for Metals) International joined forces with the National Bureau of Standards (now the National Institute of Standards and Technology) in an effort to improve the reliability of phase diagrams by evaluating the existing data on a system-by-system basis. An international programme for alloy phase diagrams was carried out. The results are available in the ASM Handbook [7], in the three-volume set of “Binary Alloy Phase Diagrams” [55], [54], in the ten-volume set of “Handbook of Ternary Alloy Phase Diagrams” [98], and in the books published by Okamoto [60], [61].

Computer software for thermodynamic calculations, e.g. MTDATA, FactSage, Thermo-Calc, are currently capable of computing phase diagrams using databases that quantify the thermodynamic properties of the materials [21], [41], [5], [18], [8], [37], [72], [70]. These programs minimise theGibbs free energy of a chemical system with respect to the portions of individual species that could possibly form. This allows the calculation of the equilibrium state and the overall composition. The calculations suggest that in general k_0^i exhibits only a very weak (< 5 %) dependence on impurity concentration up to about 1000 ppm. Currently, the standard uncertainty in the calculated values is not known, but based on the scatter observed in comparison with other determinations of k_0^i for comparable systems it is estimated to be of the order of 30 %.

The available data are sufficient for systems for which miscibility without the formation of other phases has been verified up to a few per cent or more by metallographic methods. For these systems, peculiarities should not exist at very low concentrations. On the other hand, further investigations are necessary for systems referred to as degenerate or zero-percent (“0 %”) systems [40], [85], [5], for which solubility has yet to be detected. Such systems are particularly insidious if eutectics or peritectics are formed very close to the freezing temperature of the pure host metal at impurity concentrations much smaller than 1 %, i.e. near to “0 %”. Freezing at the eutectic or peritectic formation temperature may yield a very flat freezing curve [16]. Since the phase diagrams have typically been investigated at concentrations near and in excess of one per cent, a small solubility at very low concentrations cannot be ruled out. Thermodynamic calculations are also limited by the lack of data at very low concentrations. In these cases, therefore, dedicated doping experiments are necessary as described in [1], [2], [3], [4], [43], [80], [108], [24], [73], [90], [89]. It is important to confirm that the doping experiments are not distorted by the precipitation of oxides [23], [24].

5. Chemical Analysis Methods

At present, the uncertainty estimates for chemical analyses are rarely expressed in a manner consistent with the GUM [42] and the reliability of the estimates remains a concern. Until recently, the common practice in chemical testing was to use the repeatability or reproducibility of measurements as the basis for the uncertainty assessment. This may still be the practice in many laboratories. Other sources of uncertainty include sampling effects, segregation effects within a sample, contamination of the analysis equipment, and calibration. The problems related to the chemical analysis are worsened by the possibility of subsequent contamination of the pure metal during the filling process of the fixed-point cell or from impurities leaching out of the graphite crucible when the metal is molten. Thus, uncertainties in chemical analyses (if reported at all) may be low. The magnitude of $u\left(c_{11}^{i}\right)$ may be comparable to c_{11}^{i} itself. Expanded uncertainties (coverage factor $k = 2$) for individual elements are normally within the range 20% to 300% of the nominal value. A fixed-point temperature should not be corrected when the uncertainties of the chemical analysis exceed 100%. This is because the application of the correction in this case may do more harm than good. Where the uncertainty of the impurity concentrations is large compared to other components of the overall fixed-point uncertainty budget, it is important to compute the degrees of freedom associated with the standard uncertainty of the SIE method given by Equation (10) to ensure that the expanded uncertainty can be properly computed, see Chapter 6.

To improve the situation, it is necessary to compare results obtained by different institutes using appropriate analysis methods for samples of the fixed-point materials that are of vital importance to the thermometry community. Such methods include, for instance: Atomic Absorption Spectrometry (AAS), Carrier-Gas Hot Extraction (CGHE), ElectroThermal Atomic Absorption Spectrometry (ETAAS), Glow Discharge Mass Spectrometry (GD-MS), Inductively Coupled Plasma Mass Spectrometry (ICP-MS), Instrumental Neutron Activation Analysis (INAA), and Photon Activation Analysis (PAA). Determination of the carbon content and that of dissolved gases such as oxygen and nitrogen is a significant problem. For the determination of non-metals, CGHE and PAA are suitable methods.

The current state-of-the-art approach for the determination of the impurity content of metallic fixed-point materials is GD-MS. Advantages of this technique are low limits of determination, excellent repeatability, and a direct solid sampling technique that avoids losses or contamination caused by wet chemical pretreatment. In contrast to most other techniques, it is considerably faster and results can be obtained within minutes to a few hours. Typically, about 50 to 70 different impurities (elements of the periodic table) can be determined with sufficiently low limits of detection down to the part per billion levels. The main drawback of GD-MS is the lack of a suitable and traceable calibration procedure for the quantification of low mass fractions with small uncertainty. With the current method of quantification, which is based on matrix-independent analyte-specific so-called standard relative sensitivity factors (Standard-RSFs), uncertainties between a factor of two (of the true value) and a factor of five are typically claimed. A further disadvantage of GD-MS is that it is difficult to quantify with small uncertainty for non-metals.

A cooperative effort between PTB and BAM *Federal Institute for Materials Research and Testing* was directed to developing an SI-traceable chemical analysis ofthe materials used in the fixed-point cells with sufficiently low uncertainties [35], [80], [81]. The new methodology for instrument calibration is to replace the current semi-quantitative approach by a quantitative one based on sets of doped samples with well-known impurity contents,

whose concentration values are directly traceable to the International System of Units. The characteristic difference from common practice is to carry out the chemical analysis of the fixed-point metal after the cell's freezing temperature has been determined. This allows for the inclusion of contamination and purification effects arising from the filling process, or due to contact with the carbon crucible and other parts of the fixed-point cell. Furthermore, the graphite crucible and other parts of the fixed-point cell that could possibly contaminate the fixed-point metal are also analysed. The use of synthetic standards has yielded hitherto unachieved uncertainties smaller than 30% for the majority of the detected impurities.

6. Effective Degrees of Freedom, Expanded Uncertainties, and Confidence Levels

The approach to reporting uncertainties developed in Chapter 3 proposes a paradigm shift for thermometry. A review of the report of Key Comparison CCT-K3 [51] and subsequent analysis [36] either implicitly (by omission) orexplicitly associate the Type B estimates for the impurity influences with infinite degrees of freedom. In the CCT-K3 exercise, the majority of the participants stated that the uncertainty estimate for the impurity influence was based on Raoult's law. Given the relatively large relative uncertainty of the chemical analyses on which these estimates depend, a more realistic assessment of the degrees of freedom is in order. For ease of reference, use is made here of an expression from the *Evaluation of measurement data —Guide to the Expression of Uncertainty in Measurement* (GUM) [42], with the equation numbering used therein. The approximation

$$\nu_i \approx \frac{1}{2}\left[\frac{\Delta u(x_i)}{u(x_i)}\right]^{-2} \tag{13}$$

provides a means to estimate the degrees of freedom ν_i given the relative uncertainty of $u(x_i)$, which is the quantity in large brackets. The alternative expression [19]

$$\nu_S \approx \frac{1}{2}\left[\frac{\Delta u}{u}\right]^{-2}\left[1+3\left(\frac{\Delta u}{u}\right)+1.2\left(\frac{\Delta u}{u}\right)^2\right] \tag{14}$$

focuses on the broadening of the asymmetric chi-squared distribution to choose a better Student distribution than Equation (13) for small ν.

Values of $\Delta u(x_i)$ are best obtained directly from reports of analysis, when the report gives uncertainties in the determination of x_i. In the absence of this information, the effective degrees of freedom may be estimated by examining the reproducibility of multiple, *independent* chemical analyses and other experimental evidence.

Once the degrees of freedom have been calculated, the coverage factor can be determined for a given confidence level (usually 95%). Following the form of the GUM, the expanded uncertainty is given by

$$U_{95} = t_{95}(\nu)u. \tag{15}$$

In Equation (15), $t_{95}(\nu)$ is from Student's distribution (or t-distribution) where ν defines the interval from $-t_{95}(\nu)$ to $+t_{95}(\nu)$ that encompasses 95% of the distribution.

Given the procedural difficulties in estimating t_{95} when it is likely that the degrees of freedom from Equation (13) will fall below 1, Equation (14) is recommended instead. The treatment of the uncertainty of non-normal distributions or distributions with low effective degrees of freedom is a current area of research, and the statistical tools are not yet fully developed.

This discussion is merely a reminder of how finite degrees of freedom influence a single-component uncertainty. The reader is referred to the GUM [42] for the procedure to be used when combining uncertainty components, each having their associated degrees of freedom, via the Welch-Satterthwaite formula.

7. Validation of Fixed-Point Cells

The SIE, OME and combined methods treated in Chapter 3 yield uncertainty estimates based on the analysis results obtained for specially-prepared test samples and the available data on the impurity effects. Thus, they assume that the fixed-point material within the cell is substantially similar in composition to the starting material. For the validation of the in-ingot quality of fixed-point cells, complementary techniques are useful for the following reasons:

- It is challenging to implement fully the SIE method for metallic fixed points, see Section 3.1.
- Fixed-point cells may be contaminated during the fabrication process or due to contact with the crucible, especially for fixed points at temperatures of 420 °C (zinc freezing point) and higher. But usually it is not practicable to break a cell for analysing the used ingot material.
- The impurities may be inhomogeneously distributed in the vertical and radial directions due to their segregation within the crystal or at grain boundaries and dislocations.

Thermal analysis of freezing (or melting) curves and the ERC (Estimate based on Representative Comparisons) method are appropriate for the validation of fixed-point cells. If either a thermal analysis or an ERC result in an estimated uncertainty larger than that obtained by the SIE, OME or combined methods, then it is likely that the cell has been contaminated, the chemical analysis underestimates the impurities, or the realisation methods are less than optimal.

For the application of the thermal analysis, it is important that the curves are not deformed by the thermal conditions within the furnace [80], [22], [67], [68] and that the freezing conditions are such that k_{eff}^{i} has nearly the same value as k_{0}^{i}, see Section 2.3.2. The utility of information that can be extracted from a series of complementary fixed-point realisations (like freezing/melting with/without a second interface, melting after slow/fast cooling, variations of the duration of the fixed-point curves and subsequent extrapolation, adiabatic measurements and other techniques) is currently a matter of active discussion, see [47], [88], [86], [87], [43], [58], [77], [39] and the following discussion. Generally, the flatter the freezing or melting curve, the greater the purity of the fixed-point substance, and the closer the measured fixed point will be to the correct temperature. Extrapolation of curves to the liquidus point as a function of F or $1/F$ [86] and plots of liquidus-point temperature versus freezing rate [100], [101], [106] all provide qualitative indications of purity. It should be kept in mind that a melt following a very fast (quench) freeze generally leads to a more homogeneous sample with a narrower melting range, whereas a melt following a slow freeze (which allows significant impurity segregation) will have a larger melting range, see Section 2.3.4.

Widiatmo *et al*. (2006, 2008, 2010, 2011a, 2011b), Yamazawa *et al*. (2007, 2008), and Tsai (2013) have compared the SIE method with the so-called slope analysis for different freezing points (Sn, Zn, Al, Ag). The slope analysis utilizes the fact that for $k_{0}^{i}=0$, i.e. assuming the validity of Raoult's law, the slope of the dependence of thefreezing temperature on $1/F$ is equal to the SIE at the liquidus point ($F=1$), cf. Equation (5) and Equation (9). Thus, the applicability of the slope analysis must be checked by one of the methods discussed in Chapter 3, and such thermal analysis does not estimate the uncertainty reliably. However, the investigations listed above show that even if the condition $k_{0}^{i}=0$ is not fulfilled for all detected impurities, the SIE and slope-analysis estimates may be comparable. This demonstrates that the slope analysis is useful as a means of validating fixed-point cells.

Pearce *et al.* have used four different methods to describe freezing curves of high-purity fixed-point samples:

1. In [67], a one-dimensional model of coupled solute and heat transport, based on finite element analysis, was employed to parameterise zinc freezing curves and especially impurity effects. As the shape of the predicted freezing curves are dictated primarily by the impurity effects, it was used also, in conjunction with experimental results, to determine the furnace settings for which spurious thermal effects are minimal.
2. A comparable model of coupled mass and heat transport was developed in COMSOL Multiphysics in [68]. This model agrees quantitatively with model (i) and shows in particular that the zinc freezing curve approaches the shape given by the Scheil expression (Equation (5) for one impurity with representative parameters). This finding supports the concept of parameterisation.
3. In [68], the fitting of the Scheil expression to freezing curves is examined with a set of Scheil curves constructed using chemical analyses of 32 tin, zinc, aluminium, and silver fixed-point cells. The fits were performed in two ways: a) T_{pure}, c_{11}, k_0 free parameters, b) T_{pure}, c_{11} free parameters, $k_0 = 0$ fixed. The results show that the model can be used reliably in a large number of cases to parameterise all three parameters, but the method can break down at the extremes of impurity parameter space. (The application of the Scheil equation is also discussed in [49].)
4. A relatively new technique for simulating phase transitions is the phase-field method summarized in [46]. The model is applied to understand the effect of experimental parameters – such as initiation technique and furnace homogeneity – on the measured freezing curve. Results show that Scheil-like freezing curves can be obtained with a specific furnace temperature profile, and provided that the freeze is of long duration the results are consistent with previous models and experiment.

The description of freezing curves achieved with models (i) to (iv) is certainly helpful for the validation of fixed-point cells and for monitoring possible changes during their use, but the modelling does not allow corrections of the fixed-point temperatures or uncertainties to be estimated.

The ERC method is no longer considered acceptable as the basis for estimating the uncertainty attributed to chemical impurities as it is somewhat dependent on chance, but it can assist in the validation of fixed-point cells. Differences in cell realisation temperatures are best measured by “direct comparison”, whereby two cells are simultaneously realised in identical thermal enclosures. (Recommendations for performing such cell comparisons are given by Mangum *et al.* (1999) and Widiatmo *et al*. (2010).) In fact, the comparisons can be direct comparisons of fixed-point cellswithin one laboratory. Advantages of single-laboratory comparisons are: (i) many effects other than cell variations are maintained constant and are not inappropriately interpreted as “cell impurities,” and (ii) because the cost is less, it is feasible to test many more cells. When using comparisons of cells [50], [86], [104], the cells should be manufactured from different sources of fixed-point materials, and preferably made using different procedures. Where the ERC method is employed for supplementary investigations, uncertainty budgets should identify the components that are encompassed in cell differences.

8. Overview of effects of impurities in the ITS-90 fixed-point substances

The influence of impurities on the fixed-point temperature differs substantially among the three types of fixed-point substances used in the ITS-90, namely cryogenic gases, water, and metals. The differences are manifest in the number and kind of common and effectively-acting impurities, their solubility in the melt and the solid, and in the slopes of the liquidus lines. The product of the fixed-point temperature T_{90} and the cryoscopic constant A is only weakly temperature dependent (the values range from 0.9 to 2.7), see Table 1. This suggests that, for all substances, the relative change of the realised temperature by impurities has the same order of magnitude for a given purity. The values m_1^i of the liquidus-line slopes listed in Appendix 2support this tendency. On average, the absolute influence of impurities is more than one order of magnitude larger for metals than for the cryogenic gases, and for water it is in between. The distribution coefficients k_0^i are tabulated in Appendix 2for two reasons. First, they show how purification can be achieved by zone refining. Second, for many systems, m_1^i can be estimated from k_0^i by applying Equation (6).

8.1. Effects of Impurities in Cryogenic Gaseous Fixed-Point Substances

The cryogenic fixed points of gaseous substances—the triple points of equilibrium H_2 (e-H_2), Ne, O_2 and Ar—are affected by only a limited number of impurities, distinct for each fixed-point substance. Due to the fact that many impurities do not influence the triple-point temperature, the OME method usually leads to a (considerable) overestimate. Based on the A values listed in Table 1, it follows that an impurity content of 1 ppm mole fraction would change the melting temperature by 54 μK, 60 μK, 221 μK, and 197 μK for *e*-H_2, Ne, O_2 and Ar, respectively, in the range of the melted fraction F from 20% to 100%. These values are larger than usually observed, especially for hydrogen and oxygen.

If the thermal analysis of melting curves is used to validate fixed-point cells, some peculiarities of the cryogenic gases must be considered. The Ar content in O_2 is easily underestimated by two orders of magnitude [63] since k_0^i of Ar is near to one. Thus, Equation (6) is not applicable and the melting curve is not broadened due to the redistribution of the Ar atoms, but the triple-point temperature is still depressed by the presence of Ar. A comparison of typical melting ranges of pure Ne isotopes with those of natural Ne samples suggests that at least part of the melting range of natural neon is due to isotopic fractionation. In the case of Ar, crystal defects may reduce the melting temperature significantly. Therefore, thermal analysis should be done following incomplete melting and slow refreezing, which may reduce the width of the melting range to 10 μK [105].

The present knowledge of the common impurities contained in commercial high-purity gases and their sensitivity coefficients m_1^i is reviewed for each of the four fixed-point substances in [64], [66]. For the m_1^i values, a ‘best guess’ and an uncertainty estimate based on experience are given. The values of the slopes of the liquidus and solidus lines as well as the resulting k_0^i values are considered in Appendix 2. In addition, this data is also given for the triple point of N_2, an often-used reference point in secondary scales. In the two references, further information is provided regarding chemical assays, which were available over up to three

decades, and, partly, on the solubility. The following impurities are the main elements affecting the triple-point temperature: Ne and He in H_2; He, H_2 and N_2 in Ne; Ar and N_2 in O_2; O_2 and N_2 in Ar.

8.2. Effects of impurities in water

The triple point of water (TPW) is the only fixed point for which it can be assumed that all impurities are practically insoluble in the solid phase and remain confined in the liquid phase ($k_0^i \approx 0$ for any impurity species), see *Guide* Section 2.2 *Triple Point of water*. This means that, provided the preparation of the ice mantle is slow enough toguarantee complete mixing in the liquid (see Section 2.3.1, freezing rate smaller than 10 $\mathrm{mmh^{-1}}$), Raoult's law is valid (Equation (4) in Section 2.2, see p. 7), and a plot of the measured TPW temperature versus $1/F$ allows the determination of the total impurity concentration [56]. The cryoscopic constant of water, see Table 1, corresponds to a depression of the TPW temperature at the liquidus point of 103 μK for an impurity content of 1 ppm mole fraction.

There are four main sources of impurities in the water of a TPW cell, see *Guide* Section 2.2 *Triple Point of water*: chemicals used in the cleaning and pre-conditioning of the cell; for borosilicate-glass cells, impurities dissolved from the glass; low-volatility compounds in the source water having a similar boiling point as water; residual gases in the cell water. For impurities with a high dissociation constant, the concentration can be determined by measuring the electrical conductivity of the water [9]. Ideally-pure water has a conductivity of order 5 $\mu\mathrm{Sm^{-1}}$ and the effective ionic conductivity amounts to 2 $\mathrm{mS\,m^2mol^{-1}}$, i.e. the conductivity increases by more than an order of magnitude for an impurity content of 1 ppm.

8.3. Effects of Impurities in Metallic Fixed-Point Substances

The effects of impurities are most problematic for the metallic fixed-point substances because of the large number of relevant impurity elements and the strong concentration dependence of the phase-transition temperature, see Table 1 and the data collation in Appendix 2.The values of the cryoscopic constants listed in Table 1 yield the strongesteffect for Cu of 1.2 mK for an impurity content of 1 ppm. Therefore, when collating the data, it is helpful to consider the rules governing the magnitude of the distribution coefficients and the solid solubility. These rules are summarised in this subsection.

In [70], the distribution-coefficient values were drawn from the literature (mainly doping studies), calculated using thermodynamic modelling software, or obtained from the liquidus slope by applying Equation (6). In the latter case, care was taken to ensure consistency of the units. A full set of parameters is presented in Appendix 2.The huge number of values (over 1300 binary systems, 25 different metalsolvents, solute atomic number from 1 to 94) for all metallic fixed-point substances of the ITS-90 and other metals, which are in some way linked to use as fixed points, suggests that the value of k_0^i for a particular impurity element is a function of its position in the periodic table, with a lesser dependence on the solvent. This opens up the possibility of predicting the value of k_0^i for impurity-solvent binary systems hitherto undetermined, with an uncertainty (in terms of $\log\left(k_0^i\right)$) estimated to be about 30%.

The solubility in both liquid and solid phases is often far from ideal. In particular, the solubility of the impurity in the solid solvent is governed by a large number of factors. An impurity is

dissolved in a solid when the crystal structure of the solvent remains unchanged by the addition of solutes. The solute may be incorporated in the solvent crystal lattice *substitutionally*, by direct replacement of a solvent atom in the lattice, or *interstitially*, by fitting into the space between solvent atoms. The propensity for two substances to form solid solutions is a complicated function of their chemical, crystallographic, and quantum properties, but the Hume-Rothery rules provide some basic guidelines to determine whether two substances are likely to form a solid solution [57], [109]:

Substitutional solid solution rules:

- The atomic radius of the solute atom must differ from that of the solvent by no more than 15%; if the difference is greater, the solute is likely to have low solubility.
- The crystal structures of solute and solvent must match.
- A metal will dissolve a metal of higher valency to a greater extent than one of lower valency.
- The solute and solvent should have similar electronegativity; the larger the difference, the more likely a compound will form instead.

Interstitial solid solution rules:

- Solute atoms must be smaller than interstitial sites in the solvent lattice.
- The solute and solvent should have similar electronegativity.

The situation is further complicated by the fact that, since the solid solubilities depend on the interactions between the solid solution and other phase(s), the maximum solid solubilities are not necessarily parameters that accurately indicate the relative compatibilities of the solute elements with the solvent element in solid solution [94]. Nonetheless, the above rules provide useful guidance on which parameters to investigate. Darken-Gurry diagrams [17], where the electronegativity of the solvent element and each impurity element is plotted as a function of the covalent radius, allow a qualitative prediction of solid solubility: on such plots, an ellipse having a width of 30% of the value of the covalent radius of the solvent element and a height of 0.8 units in electronegativity may be drawn, as per the prescription of Darken and Gurry, to reflect the fact that impurity elements closer to the solvent element on such a diagram are expected to have higher solid solubility.

References

[1] Ancsin J 2001 *Metrologia* **38** 229-235

[2] Ancsin J 2003 *Metrologia* **40** 36-41

[3] Ancsin J 2007 *Metrologia* **44** 303-307

[4] Ancsin J 2008 *Metrologia* **45** 16-20

[5] Andersson J O, Helander T, Höglund L, Shi P F, Sundman B 2001 *CALPHAD* **26** pp. 273

[6] Atkins P W 1978 *Physical chemistry* (University Press, Oxford) ISBN 0-19-855148-7

[7] Baker H(ed.) 1992 *ASM Handbook, Volume 3, Alloy Phase Diagrams* (ASM International, Materials Park Ohio)

[8] Bale C W,Chartrand P, Degterov S A, Eriksson G, Hack K, Ben Mahfoud R, Melançon J, Pelton A D, Petersen S 2002 *CALPHAD* **26** pp. 189

[9] Ballico M 1999 *Meas. Sci. Technol.* **10** L33-L36

[10] Bloembergen P, Yamada Y 2006 *Metrologia* **43** 371-382

[11] Bloembergen P, Dong W, Bai C, Wang T 2011 *Int. J. Thermophys.* **32** 2633-2656

[12] Bongiovanni G, Crovini L, Marcarino P 1975 *Metrologia* **11** 125-132

[13] Brice J C 1973 *The Growth of Crystals from Liquids* (North-Holland Publishing Company, Amsterdam)

[14] Burton J A, Prim R C, Slichter W P 1953 *J. Chem. Phys.* **21** 1987

[15] Chernov A A 1984 *Modern Crystallography III Crystal Growth* (Springer-Verlag, Berlin)

[16] Connolly J J, McAllan J V 1980 *Metrologia* **16** 127-132

[17] Darken L S, Gurry R W 1953 *Physical Chemistry of Materials* (McGraw-Hill, New York)

[18] Davies R H, Dinsdale A T, Gisby J A, Robinson J A J, Martin S M 2002 *CALPHAD* **26**(2) 229

[19] Douglas R J 2005 Private Communication

[20] Drápala J, Kuchař L 2008 *Metallurgy of Pure Metals* (Cambridge International Science Publishing, Cambridge)

[21] Eriksson G, Hack K 1990 *Metallurgical Transactions B* **21B** 1013-1023

[22] Fahr M, Rudtsch S 2008 *Int. J. Thermophys*. **29** 126-138

[23] Fahr M, Rudtsch S 2009 *Metrologia* **46** 423-438

[24] Fahr M, Rudtsch S, Aulich A 2011 *Int. J. Thermophys*. **32** 2239-2251

[25] Fellmuth B 2003 "Comments on the underestimation of the change of fixed-point temperatures by impurities due to a non-justified application of Raoult's law" *BIPM Com. Cons. Thermométrie **22**, Document* CCT/03-12(http://www.bipm.org/cc/CCT/Allowed/22/CCT03-12.pdf)

[26] Fellmuth B, Fischer J, Tegeler E 2001 "Uncertainty budgets for characteristics of SPRTs calibrated according to the ITS-90" *BIPM Com. Cons. Thermométrie **21**, Document CCT/01-02* (http://www.bipm.org/cc/CCT/Allowed/21/CCT01-02.pdf)

[27] Fellmuth B, Hill K D 2006 *Metrologia* **43** 71-83

[28] Fellmuth B, Tegeler E, Fischer J 2005 „Uncertainty of the characteristics of SPRTs calibrated according to the ITS-90" *Proc. 9th Symposium on Temperature and Thermal Measurements in Industry and Science*, ed. D. Zvizdić, L.G. Bermanec,T. Veliki and T. Stašić (IMEKO / University of Zagreb, Faculty of Mechanical Engineering and Naval Architecture, Zagreb) pp. 1135-1140

[29] Fellmuth B, Wolber L 2011 *Int. J. Thermophys*. **32** 161-172

[30] Furukawa G T, Piccirelli J H, Reilly M L 1984 *Purity Determinations by Thermal Methods, ASTM STP 838*, ed. R.L. Blaine, C.K. Schoff (ASTM, Philadelphia) pp.90-106

[31] Furukawa G T 1986 *J. Res. Natl. Bur. Stand.* **91** 255-275

[32] Gilman J J (ed.) 1963 *The Art and Science of Growing Crystals* (John Wiley & Sons, New York)

[33] Guggenheim E A 1949 *Thermodynamics, An Advanced Treatment for Chemists and Physicists* (Interscience, New York)

[34] Gulliver G H 1913 *J. Inst. Met.* **9** 120

[35] Gusarova T 2010 "Wege zur genauen Charakterisierung hochreiner Materialien mit der Glimmentladungs-Massenspektrometrie(GD-MS)" *Thesis, BAM-Dissertationsreihe, Vol.* **55** (BAM,Berlin) (http://www.bam.de/de/service/publikationen/dissertationen_51_100.htm)

[36] Guthrie W F2002 "Should $(T_1 - T_2)$ have larger uncertainty than T_1?" *Proc. 8th Symposium on Temperature and Thermal Measurements in Industry and Science*, ed. B. Fellmuth, J. Seidel and G. Scholz (VDE Verlag GmbH, Berlin) ISBN 3-8007-2676-9 pp. 887-892

[37] Head D I, Davies H, Gray J, Quested P 2008 *Int. J. Thermophys.* **29** 1796-1807

[38] Hein K, Buhrig E (ed.) 1983 *Kristallisation aus Schmelzen* (Deutscher Verlag für Grundstoffindustrie, Leipzig)

[39] Hill K D 2014 *Int. J. Thermophys.* **35** 636-647

[40] Hume-Rothery W, Anderson E 1960 *Phil. Mag.* **5** 383

[41] Jansson B, Jönsson B, Sundman B, Ågren J 1993 *Thermochim. Acta* **214** 93-96

[42] JCGM 2008 *Evaluation of measurement data—Guide to the Expression of Uncertainty in Measurement* (Joint Committee for Guides in Metrology) http://www.bipm.org/utils/common/documents/jcgm/JCGM_100_2008_E.pdf

[43] Jimeno-Largo P, Bloembergen P, Ancsin J 2005 „An experimental and theoretical analysis of the effect of impurities on the adiabatic melting curve of silver" *Proc. 9th Symposium on Temperature and Thermal Measurements in Industry and Science*, ed. D. Zvizdić, L.G. Bermanec, T. Veliki and T. Stašić (IMEKO / University of Zagreb, Faculty of Mechanical Engineering and Naval Architecture, Zagreb) pp 233-238

[44] Krapf G, Mammen H, Blumröder G, Fröhlich T 2012 *Meas. Sci. Technol.* **23** 074022

[45] Kurz W, Fisher D J 1998 *Fundamentals of Solidification*, 4th edition (Trans Tech Publications Ltd, Uetikon-Zuerich)

[46] Large M J, Pearce J V 2014 *Int. J. Thermophys*. **35** 1109-1126

[47] Lee H K, Gam K S 1992 "An assessment of the quality of freezing point samples by freezing and melting experiments" *Temperature: Its Measurement and Control in Science and Industry, Vol. 6,* ed. J. F. Schooley (AIP, New York) pp 327-331

[48] Lewis G N, Randall M, Pitzer K S, Brewer L 1961 *Thermodynamics* (McGraw-Hill, New York)

[49] Malik Z, Hunt J D, Davies H, Lee P D, Lowe D, Quested P N 2011 *Int. J. Thermophys.* **32** 1589-1601

[50] Mangum B W, Bloembergen P, Chattle M V, Fellmuth B, Marcarino P, Pokhodun A I 1999 *Metrologia* **36** 79-88

[51] Mangum B W, Strouse G F, Guthrie W F, Pello R, Stock M, Renaot E, Hermier Y, Bonnier G, Marcarino P, Gam K S, Kang K H, Kim Y-G, Nicholas J V, White D R, Dransfield T D, Duan Y, Qu Y, Connolly J, Rusby R L, Gray J, Sutton G J M, Head D I, Hill K D, Steele A, Nara K, Tegeler E, Noatsch U, Heyer D, Fellmuth B, Thiele-Krivoj B, Duris S, Pokhodun A I, Moiseeva N P, Ivanova A G, de Groot M J, Dubbeldam J F 2002, *Metrologia* **39** 179-205

[52] Mangum B W, Bloembergen P, Chattle M V, Fellmuth B, Marcarino P, Pokhodun A I 2000 "Optimal realization of the defining fixed points of the ITS-90 that are used for contact thermometry" *BIPM Com. Cons. Thermométrie **20**, Document CCT/2000-13* (This document is available on request from the BIPM.)

[53] Mangum B W, Furukawa G T 1990 *NIST Tech. Note 1265* (U.S. Government Printing Office, Washington)

[54] Massalski T B (ed.) 1996 *Binary alloy phase diagrams*, 2nd edition, plus updates on CD ROM (ASM International, Materials Park Ohio)

[55] Massalski T B (editor-in-chief), Okamoto H, Subramanian P R, Kacprzak L (editors) 1990 *Binary alloy phase diagrams*, 2nd edition (ASM International, Materials Park Ohio)

[56] Mendez-Lango E 2002 "A non-destructive method to evaluate the impurity content in triple point of water cells", *Proc. 8th Symposium on Temperature and Thermal*

Measurements in Industry and Science, ed. B. Fellmuth, J. Seidel, G. Scholz (VDEVerlag GmbH, Berlin) pp. 465-470

[57] Mizutani U 2010 *Hume-Rothery Rules for Structurally Complex Alloy Phases* (CRC Press, ISBN 978-1420090581)

[58] Morice R, Bonnier G, Barbaras J C, Fleurence N, Le Sant V, Ridoux P, Filtz J R 2008 *Int. J. Thermophys*. **29** 1785-1795

[59] Nubbemeyer H G, Fischer J 2002 *Metrologia* **39** Tech. Suppl. 03001

[60] Okamoto H2000 *Desk Handbook, Phase Diagrams for Binary Alloys* (ASM International, Materials Park Ohio) ISBN 0-87170-682-2

[61] Okamoto H 2002 *Phase Diagrams of Dilute Binary Alloys* (ASM International, Materials Park Ohio) ISBN 0-87170-761-6

[62] Papon P, Leblond J, Meijer P H E 2006 *The Physics of Phase Transitions* (Springer-Verlag, Berlin)

[63] Pavese F, Ferri D, Giraudi D 1988 *Adv. Cryog. Eng.* **33** 1039-43

[64] Pavese F 2009 *Metrologia* **46** 47-61

[65] Pavese F 2011 *Metrologia* **48** 268-274

[66] Pavese F, Molinar Min Beciet G 2013 *Modern Gas-Based Temperature and Pressure Measurements* (Springer Science + Business Media, New York)

[67] Pearce J V, Veltcheva R I, Lowe D H, Malik Z, Hunt J D 2012 *Metrologia* **49** 359-367

[68] Pearce J V 2013 "A coupled heat and mass transfer model of pure metal freezing using COMSOL Multiphysics" *Temperature: Its Measurement and Control in Science and Industry, Vol.**8**, AIP Conf. Proc. 1552*, ed. C. W. Meyer (AIP Publishing LLC,Melville, New York) pp. 289-294

[69] Pearce J V, Veltcheva R I, Large M J 2013 "Impurity and thermal modelling of SPRT fixed-points" *Temperature: Its Measurement and Control in Science and Industry, Vol. **8**, AIP Conf. Proc. 1552*, ed. C. W. Meyer (AIP Publishing LLC, Melville,New York) pp. 283-288

[70] Pearce J V 2014 *Int. J. Thermophys*. **35** 628–635

[71] Pearce J V, Gisby J A, Steur P P M 2016 *Metrologia* **53** 1101-1114

[72] Petchpong P, Head D I 2011a *Int. J. Thermophys*. **32**, 1507-1517

[73] Petchpong P, Head D I 2011b *Int. J. Thermophys.* **32** 1525-1534

[74] Pfann W G 1966 *Zone Melting* (John Wiley and Sons, New York)

[75] Pimpinelli A, Villain J 1998 *Physics of Crystal Growth* (Cambridge University Press, Cambridge)

[76] Prince A 1966 *Alloy Phase Equilibria* (Elsevier, Amsterdam)

[77] Renaot E, Valin M H, Elgourdou M 2008 *Int. J Thermophys* **29** 852-860

[78] Ripple D, Pokhodun A, Steur P, Strouse G and Tamura O 2008 "Recommended List of Common Impurities for Metallic Fixed-point Materials of the ITS-90" *BIPM Com. Cons. Thermométrie **24**, Document* CCT/08-16/rev(http://www.bipm.org/cc/CCT/Allowed/24/D16_rev_RippleCommonImpuritiesTa blesB.pdf)

[79] Rudtsch S 2005 "Cryoscopic Constant, Heat and Enthalpy of Fusion of Metals and Water" *BIPM Com. Cons. Thermométrie **23**, Document CCT/05-04/rev* (http://www.bipm.org/cc/CCT/Allowed/23/CCT_05_04_rev.pdf)

[80] Rudtsch S, Fahr M, Fischer J, Gusarova T, Kipphardt H, Matschat R 2008 *Int. J. Thermophys* **29** 139-150

[81] Rudtsch S,Gusarova T, Aulich A, Fahr M, Fischer J, Kipphardt H, Matschat R, Panne U 2011 *Int. J. Thermophys.* **32** 293-302

[82] Scheil E 1942 *Z. Metallk.* **34** 70-72

[83] Sloan G J, McGhie A R 1988 *Techniques of Melt Crystallisation* (John Wiley & Sons, New York)

[84] Smith V G, Tiller W A, Rutter J W 1955 *Can. J. Phys.* **33** 723-745

[85] Stølen S, Grønvold F 1999 *J. Chem. Thermodynamics* **31** 379-398

[86] Strouse G F 2003 "NIST Methods of Estimating the Impurity Uncertainty Component for ITS-90 Fixed-Point Cells from the Ar TP to the Ag FP" *BIPM Com. Cons. Thermométrie **22**, Document CCT/03-19* (http://www.bipm.org/cc/CCT/Allowed/22/CCT03-19.pdf)

[87] Strouse G F 2005 "NIST certification of ITS-90 fixed-point cells from 83.8058 K to 1234.93 K: Methods and Uncertainties" *Proc. 9th Symposium on Temperature and Thermal Measurements in Industry and Science*, ed. D. Zvizdić, L.G. Bermanec,T. Veliki and T. Stašić (IMEKO / University of Zagreb, Faculty of Mechanical Engineering and Naval Architecture, Zagreb) pp. 879-884

[88] Strouse G F, Moiseeva N P 1999 "Tin freezing-point standard – SRM 741a" *NIST Special Publication 260-138* (U.S. Government Printing Office, Washington)

[89] Sun J, Rudtsch S 2014 *Int. J. Thermophys.* **35** 1127–1133

[90] Tabacaru C, Gómez E, del Campo D 2011 *Int. J. Thermophys.* **32** 1563-1572

[91] TA-ITS-90 2017 *Technical Annex for the International Temperature Scale of 1990 (ITS-90)* (http://www.bipm.org/utils/en/pdf/MeP_K_Technical_Annex.pdf)

[92] Tiller W A, Jackson K A, Rutter J W, Chalmers B 1953 *Acta Metallurgica* **1** 428-437

[93] Tiller W A, Sekerka R F 1964 *J. Appl. Phys.* **35** 2726-2729

[94] Trumbore F A 1960 *The Bell System Technical Journal* January 205-233

[95] Tsai S F 2013 "Thermal analysis on the realization of the tin fixed point" *Temperature: Its Measurement and Control in Science and Industry, Vol. **8**, AIP*

Conf. Proc. 1552,ed. C. W. Meyer (AIP Publishing LLC, Melville, New York) pp. 255-258

[96] Ubbelohde A R 1965 *Melting and Crystal Structure* (Clarendon press, Oxford)

[97] Verhoeven J D, Heimes K A 1971 *J. Crystal Growth* **10** 179-184

[98] Villars P, Prince A, Okamoto H 1995 *Handbook of ternary alloy phase diagrams* (ASM International, Materials Park Ohio)

[99] Weinstein L, Adam J A 2008 *Guesstimation* (University Press, Princeton) ISBN 978-0-691-12949-5

[100] Widiatmo J V, Harada K, Yamazawa K, Arai M 2006 *Metrologia* **43**, 561-572

[101] Widiatmo J V, Harada K, Yamazawa K, Arai M 2008 *Int. J. Thermophys*. **29** 158-170

[102] Widiatmo J V, Harada K, Yamazawa K, Tamba J, Arai M 2011a *Int. J. Thermophys.* **32** 2281-2294

[103] Widiatmo J V, Sakai M, Satou K, Yamazawa K, Tamba J, Arai M 2011b *Int. J. Thermophys.* **32** 309-325

[104] Widiatmo J V, Yamazawa K, Tamba J, Arai M 2010 "Direct Cell Comparison for Evaluation of Impurity Effect in Fixed-Point Realization" *BIPM Com. Cons. Thermométrie **25**, Document CCT/10-22* (http://www.bipm.org/cc/CCT/Allowed/25/D22_Direct_Cell_Comparison_(NMIJ)_revised.pdf)

[105] Wolber L, Fellmuth B 2008 *Int. J. Thermophys*. **29** 82-92

[106] Yamazawa K, Widiatmo J V, Arai M 2007 *Int. J. Thermophys.* **28** 1941-1956

[107] Yamazawa K, Widiatmo J V, Tamba J, Arai M 2008 "Limits of the SIE and the thermal analysis on impurity effect evaluation" *BIPM Com. Cons. Thermométrie **24**, Document CCT/08-03* (http://www.bipm.org/cc/CCT/Allowed/24/D03_CCT-WG3_Yamazawa.pdf)

[108] Zhang J, Rudtsch S, Fahr M 2008 *Int. J. Thermophys.* **29** 151-157

[109] Zhang Y M,Evans J R G, Yang S 2010 *Journal of Crystallization Physics and Chemistry* **1** 81